Available online at www.sciencedirect.com
ScienceDirect
Ceramics International 35 (2009) 665–671
CERAMICS INTERNATIONAL
www.elsevier.com/locate/ceramint

Microstructure and chemical degradation of adobe and clay bricks

Juliana A. Calabria [a], Wander L. Vasconcelos [a], Aldo R. Boccaccini [b,*]

[a] Federal University of Minas Gerais, Department of Metallurgical and Materials Engineering, Belo Horizonte, Brazil
[b] Imperial College London, Department of Materials, London SW7 2 BP, UK

Received 3 September 2007; received in revised form 3 January 2008; accepted 30 January 2008
Available online 24 April 2008

Abstract

The environmental degradation of adobe and fired clay brick was studied. Leaching media based on $Na_2S_2O_5$ solution and deionized water were used. The microstructure of the samples was evaluated by X-ray powder diffraction, nitrogen adsorption–desorption (BET method), Fourier transform infrared spectroscopy and scanning electron microscopy. The predominant phases detected were kaolinite and quartz for both the adobe and fired brick samples. The high surface reactivity, associated with a large amount of OH groups, contributes to the significant degradation of adobe. The fired clay brick showed a significant decrease in the average pore diameter after the first day of the leaching process; its specific surface area exhibited a reduction of about three orders of magnitude. The results of the present investigation contribute to a better understanding of the correlation between structure and leaching behaviour in adobe and clay brick, attending the renewed interest in these materials as environmentally attractive building blocks.
© 2008 Elsevier Ltd and Techna Group S.r.l. All rights reserved.

Keywords: B. Microstructure; B. Porosity; D. Clays; E. Structural applications; Adobes

1. Introduction

Although red ceramics (structural clay products) have been in use since ancient times, knowledge about the quantitative correlations between microstructure, properties and performance in actual applications is still limited [1].

Adobe is an ancient form of brick which consists of earth (mud, silt and sand) and water. Occasionally, straw is also present in the structure to enhance mechanical resistance. Adobe does not go through a firing process; instead, it is submitted to a prolonged period of drying, usually carried out by exposing the material to the sunlight. An adobe building can last hundreds of years and it is totally recyclable [2,3]. This explains the current interest in adobe as environmental friendly material for sustainable construction [4]. Adobe is a porous material and acts as humidity regulator; it is capable of accumulating up to 30 times more humidity than a regular fired brick. It is permeable and it can function as an air filter, fresh air comes inside, while used air escapes out through the walls [2]. Hence, the amount, size and distribution of pores are directly related to these properties. Porosity is one of the factors that influence the chemical reactivity of solids and the physical–chemical interaction between the solids and the gases and liquids that may percolate the material; porosity also determines the resistance to degrading agents and, therefore, it influences the structural integrity and durability of materials [3].

In particular, in adobe, water sorption occurs in direct relation to its porosity. The pore size and pore distribution determine the degree of water sorption [1,5]. The capillary effect, due to the presence of pores in the microstructure, has remarkable importance when it comes to degradation by humidity, which is a limiting factor for a wider use of adobe [6,7]. When a solution contacts a clay surface, an ion exchange mechanism is established which is dependant on the ion concentration, pH and presence of other ions [8]. In acid solution, hydration of repulsive forces present in the clay surfaces are removed due to diffusion of H^+ ion in the inner layers, which neutralizes the hydroxyl groups. The chemical attack starts with the sorption of the acid on the solid surface, causing the substitution of exchangeable cations by protons. A chemical reaction takes place and the products of the reaction solution are desorbed into the liquid phase [9,10].

The overall goal of the present investigation is to increase knowledge about the behaviour of clay brick and adobe under

* Corresponding author.
E-mail address: a.boccaccini@imperial.ac.uk (A.R. Boccaccini).

0272-8842/$34.00 © 2008 Elsevier Ltd and Techna Group S.r.l. All rights reserved.
doi:10.1016/j.ceramint.2008.01.026

different environmental conditions. The study of porosity is particularly relevant because, as mentioned above, porosity directly influences the material durability and performance during its useful lifetime, having impact on the technical, economic and aesthetical aspects. Thus, the specific objective of this study was to evaluate and compare the behaviour of adobe and fired brick submitted to leaching processes, and to correlate the processing characteristics, properties and microstructure of both materials.

2. Experimental procedure

2.1. Materials

We used in this investigation adobe, fired brick and clay from Minas Gerais (Brazil). Clays are denominated A and B, which were used to fabricate adobe and fired brick, respectively.

Clay A has as major components (wt%): SiO_2 (33.8%), Al_2O_3 (26.7%), Fe_2O_3 (21.5%). The chemical composition of clay B is: SiO_2 (86%), Al_2O_3 (9.2%), Fe_2O_3 (3%). The adobe was fabricated by drying the material under sunlight while the fired brick was heat treated at around 600 °C. In the case of fired brick, local producers are usually located close to a source of clay. The clay mass to produce the fired brick is normally mixed with water and sand and the mixture is then used in an extrusion machine to shape the blocks. Subsequently the bricks are heat treated in ovens for a period of about 1 day at temperatures of ~600 °C. The blocks are then dried in air. The typical process for adobe manufacturing is much simpler: the mud mass (water and clay) is prepared and shaped manually. After shaping the blocks, these are placed on a planar surface and left to dry under the sunlight. For the present investigation commercial fired bricks (Cerâmica Abelha, Minas Gerais, Brazil) of dimensions 23 cm × 10 cm × 5 cm were used while the dimensions of the adobe used were 24 cm × 13 cm × 13 cm.

2.2. Characterization

Fourier transform infrared spectroscopy (FTIR) was used to identify organic and inorganic groups. The equipment employed was a PerkinElmer (model Paragon-1000). The method used was diffuse reflectance and the samples were prepared as powders. In order to obtain the infrared spectra, 0.002 g of the material (fired brick or adobe) and 0.2 g of KBr (potassium bromide) were used. They were dried at 100 °C for about 4 h.

The instrument used for scanning electron microscopy (SEM) was a JEOL, model JSM-5410. Fired brick and adobe samples were prepared by ceramography and coated with a gold film.

X-ray diffraction (XRD) analyses were carried out using a Phillips diffractometer, model PW-3710, with Cu Kα radiation.

For physical nitrogen sorption analysis (Autosorb-1, Quantachrome) samples were powdered after crushing. Initially, the material was degassed at 120 °C. The BET method (nitrogen sorption at 77 K) was used to obtain the specific surface area, specific volume and pore size distribution of adobe and fired brick samples.

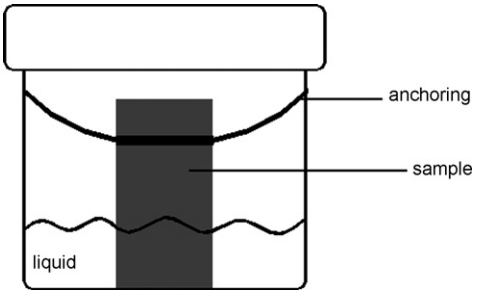

Fig. 1. Schematic diagram showing the set up used for the degradation (leaching) experiment.

2.3. Degradation evaluation

A 0.001 M $Na_2S_2O_5$ solution (from now on referred to as ''Na–S solution'') was prepared in order to obtain an aggressive medium (with a similar effect of acid rain) to investigate degradation of the materials. The sodium metasulphite ($Na_2S_2O_5$) is commonly used as a sulphur standard [11]. According to literature the pH of acid rain lies between 5 and 5.6 [12], while the measured pH of our solution was 5.

The prepared test bodies (fired clay brick and adobe) had a rectangular shape of about 2 cm × 1 cm × 1 cm. The simulation itself was made by using two degrading media: the first one containing 7 mL $Na_2S_2O_5$ and the second one with 7 mL of deionized water. They were kept in separate recipients and submitted to an ''anchorage'' to prevent them from tumbling inside the recipient, as shown schematically in Fig. 1. After the experiment, the liquid was removed by simple filtration and the leached material was dried in air at 60 °C for at least 2 days.

3. Results and discussion

3.1. Phase identification

Figs. 2 and 3 show the XRD patterns of the materials investigated showing a predominance of quartz and kaolinite for the clays A and B and for the fired brick and adobe samples. Clay A was used to fabricate adobe, while clay B was the raw-material for the fired brick. The XRD spectrum of the fired

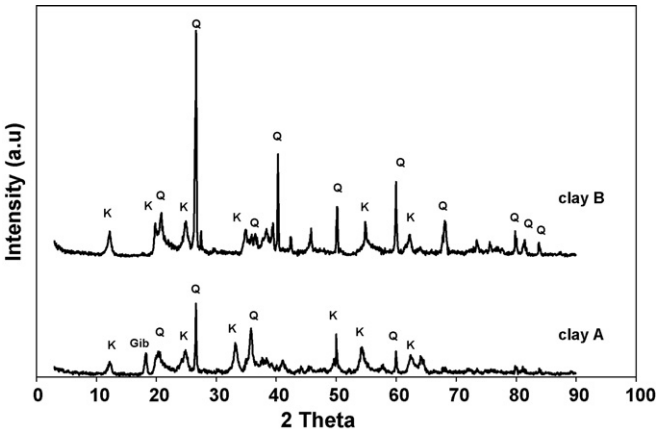

Fig. 2. X-ray powder diffraction patterns for clays A and B. The detected predominant crystalline phases are: kaolinite (K), quartz (Q) and gibbsite (Gib).

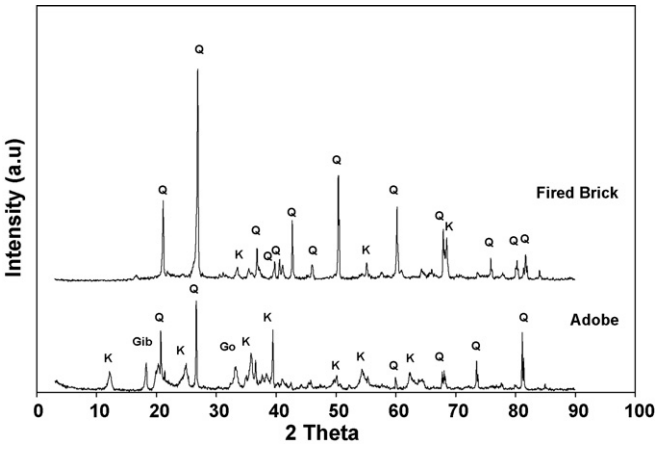

Fig. 3. X-ray powder diffraction patterns for adobe and fired brick. The detected predominant crystalline phases are: kaolinite (K), quartz (Q), gibbsite (Gib) and goethite (Go).

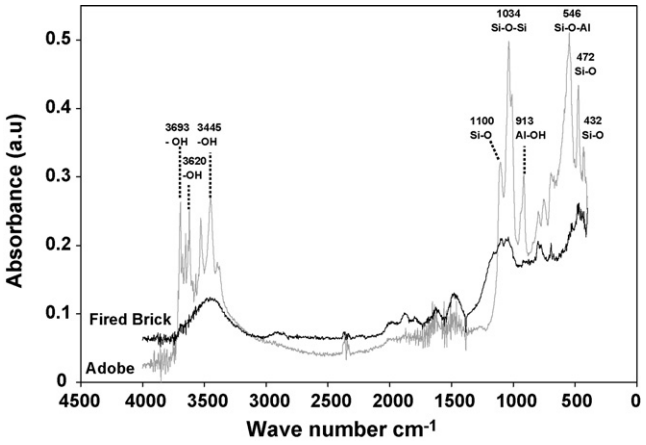

Fig. 4. FTIR spectra for adobe and fired brick samples.

brick shows traces of kaolinite phase. This can be explained by the low firing temperature used in this process [13], which is common to a large number of local Brazilian clay brick industries. For the adobe specimen the XRD spectrum remains almost the same as that of the starting clay, which follows from the room temperature treatment used in the drying process. The quartz phase is due to sand addition during the fabrication process, which results in improved mechanical resistance.

The FTIR spectrum for the adobe sample (Fig. 4) shows a large amount of OH groups. For the spectrum of fired brick (also shown in Fig. 4), the peaks associated to water absorption appear less intense than in the adobe sample. In the spectra of both ceramics it is possible to observe absorption bands corresponding to the Si–O–Si, Si–O and Si–O–Al bonds.

Figs. 5–8 show SEM micrographs of selected samples and Figs. 5 and 6 show results of EDS (energy dispersive spectrometry) analyses. The SEM image in Fig. 5(a) shows the presence of two microstructural features in fired brick. In the region labelled 1 there is a lamellar feature with impregnated crystals on the surface. In the rest of the specimen larger grains can be observed. The formation of such grains is due to sintering, which promotes the coalescence of particles. We also observed that porosity is uniformly distributed throughout the sample. The SEM image in Fig. 6(a) shows

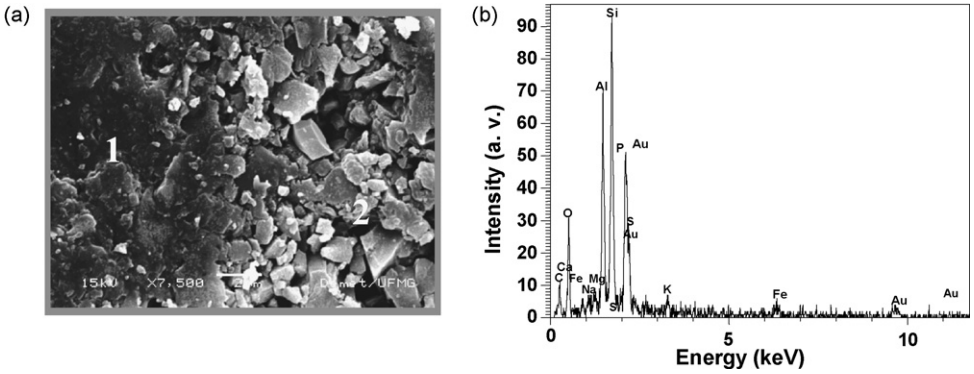

Fig. 5. (a) SEM micrograph of the fired brick sample, showing (1) lamellar structure, (2) larger equiaxed grains. (b) EDS spectrum for the image (a).

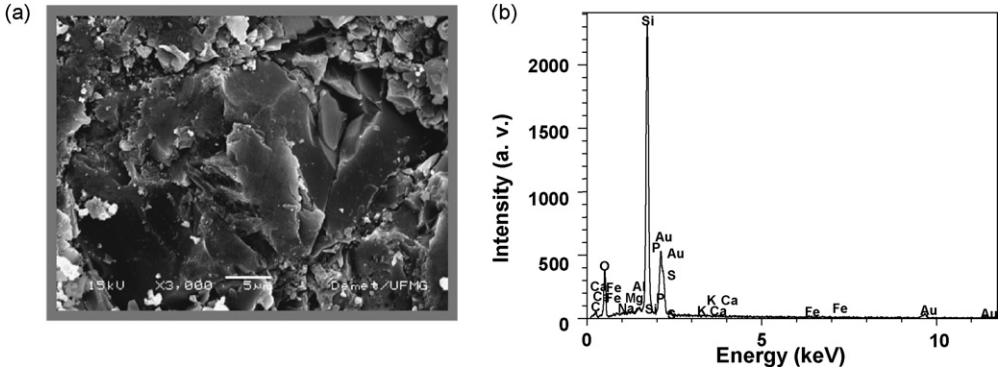

Fig. 6. (a) SEM micrograph of the fired brick sample and (b) EDS spectrum from image (a).

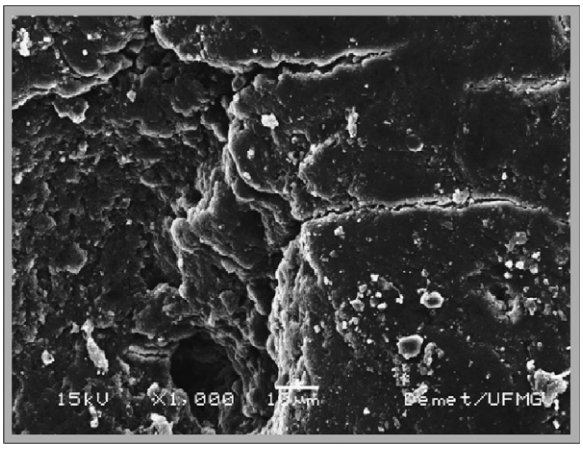

Fig. 7. SEM micrograph of an adobe sample, showing lamelar structure.

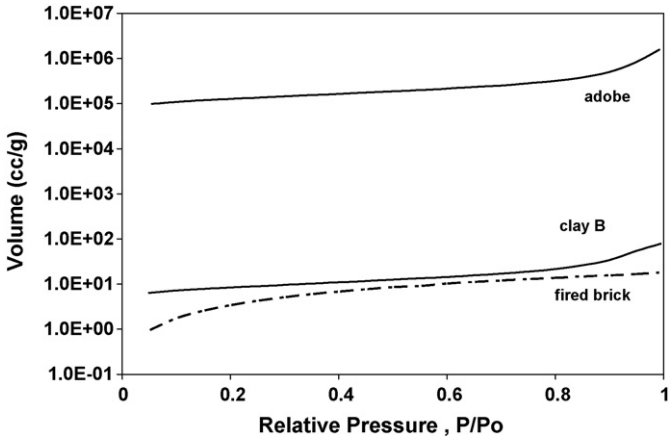

Fig. 9. Nitrogen adsorption isotherms for the adobe, clay B and fired brick samples.

even larger grains. Through EDS (Figs. 5(b) and 6(b)) a larger amount of Si in the regions with rounded aspect were identified, which suggests that those grains correspond to the quartz phase, in agreement with the XRD results.

The adobe sample shows a microstructure that points to a more fragile structure than that of fired brick. The layered morphology of adobe shown in Fig. 7 suggests a low mechanical strength, since the regions between the layers can be displaced more readily.

The difference between the adobe and fired brick samples is further illustrated comparing Figs. 6 and 8 which show different grain sizes and morphologies. Fig. 8 (adobe sample) shows crystal clusters spread over the surface, while the surface of the fired brick (Fig. 7) suggests a more compacted structure which comes from the stronger bonds between grains formed during firing.

3.2. Porosity investigation

The water absorption in a material can be related to its porosity. Moreover, the average pore size and pore size distribution influence the amount of water that the material absorbs [14,15]. Hence, pore volume and structure are significant parameters dictating the leaching behaviour of materials [16,17]. Furthermore, porosity is one of the major causes of the low mechanical strength of ceramic materials. For adobe, the issue of poor mechanical properties [18] is even more evident and serious; this is not only because of porosity but also due to the weak bonds between particles.

Fig. 9 shows the nitrogen adsorption isotherms of clay B, adobe and fired brick samples. It is observed that the volume of nitrogen incorporated into the pores of the adobe sample is four orders of magnitude larger than that in clay B. Nitrogen volume adsorbed into the pores of clay B is one order of magnitude larger than that for the fired brick. These results confirm that porosity in adobe is the highest. The lower porosity observed for fired brick is consistent with the sintering process to which this material was submitted. Results are not shown for clay A because they are quite similar to clay B.

The pore size distribution (by volume) is presented in Fig. 10, which shows the higher porosity of the adobe sample when compared to clay B and the fired brick sample. It is also observed that the pores in the adobe and clay B samples have a certain regularity in size.

The specific surface area (S_p), the specific pore volume (V_p) and the average pore diameter (D_p) of the different materials investigated are presented in Table 1. These data show that the nanoporosity in adobe is higher than that in fired brick.

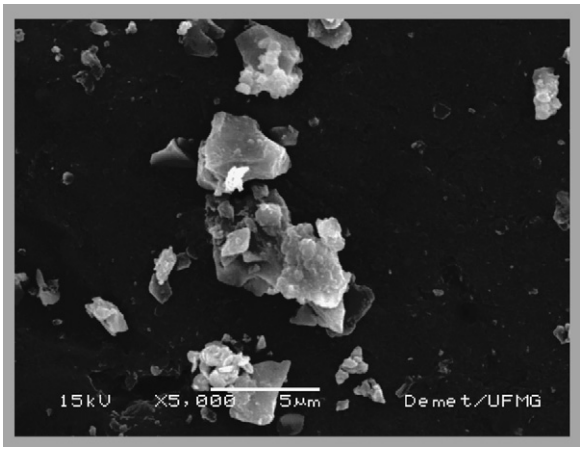

Fig. 8. SEM micrograph of an adobe sample at higher magnification.

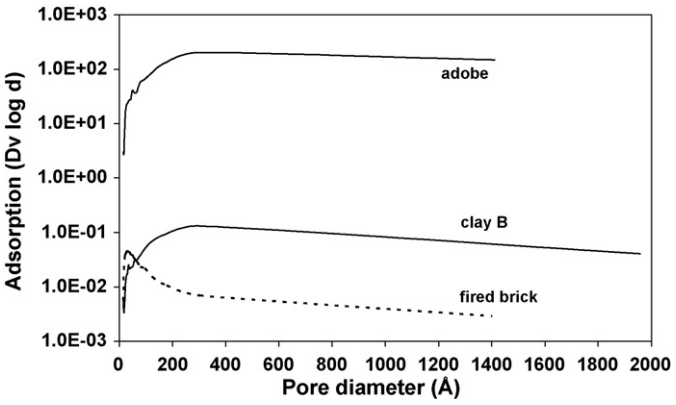

Fig. 10. Pore size distribution for clay B, adobe and fired brick.

Table 1
Specific surface area (S_p), specific pore volume (V_p) and average pore diameter (D_p) of samples investigated

Sample	S_p (m^2/g)	V_p (cm^3/g)	D_p (nm)
Clay A	61	0.294	19.2
Clay B	29	0.122	16.5
Adobe	44	0.243	21.8
Fired brick	28	0.028	4.0

Moreover, the results of nitrogen sorption confirm the high porosity of adobe and indicate the decrease in porosity as the clay is transformed into a fired ceramic. The data also show that the pore size distribution in the fired brick is relatively broad, with pore size mostly below 20 nm (Fig. 10).

Fig. 11(a) shows particles of clay B, in which the lamellar morphology (sheet structure) is observed, while Fig. 11(b) shows a region of a fired brick sample. Comparing Fig. 11(a) and (b) it is confirmed that the dispersed grains (lamellar structure) of the clay are modified giving a compact structure after sintering. As expected, the clay particles become more strongly bonded upon firing leading to a denser material with enhanced mechanical properties and higher resistance to the action of degrading agents.

Although the mechanical properties of adobe and fired brick were not measured in this study, it is well known that adobe has usually lower fracture strength than fired brick [18]. Moreover, according to the literature, the mechanical properties of adobe depend from the region where it is made as well as on the type of clay [18,19]. Typical values of the compressive strength and modulus of rupture are ~2 MPa and ~0.30 MPa, respectively, e.g. for adobes from New Mexico [19], while average Young's modulus values of 90 MPa have been determined on adobe [20].

3.3. Leaching process

The leaching process in adobe and fired brick was evaluated using deionized water and a Na–S solution at different time intervals. After leaching, the materials presented a loss of structural integrity, and it was possible to compare degradation aspects of the fired brick and adobe samples. FTIR was used to evaluate the presence of adsorbed and structural water. These experiments were also used to indirectly evaluate the surface reactivity of the ceramics, with the results shown in Figs. 12–15. Tables 2 and 3 present nitrogen adsorption–desorption values for specific surface area, specific pore volume, and average pore diameter for different leaching time intervals, for the adobe and fired brick samples, respectively.

Figs. 12 and 13 show adsorption bands corresponding to OH groups at different wave number ranges. Characteristic absorption bands of Si–OH groups in the region between 950 cm^{-1} and 1200 cm^{-1} are observed, especially for adobe (curve (i)). In the fired brick sample, such adsorption bands are less intense; indicating that part of the structural water was

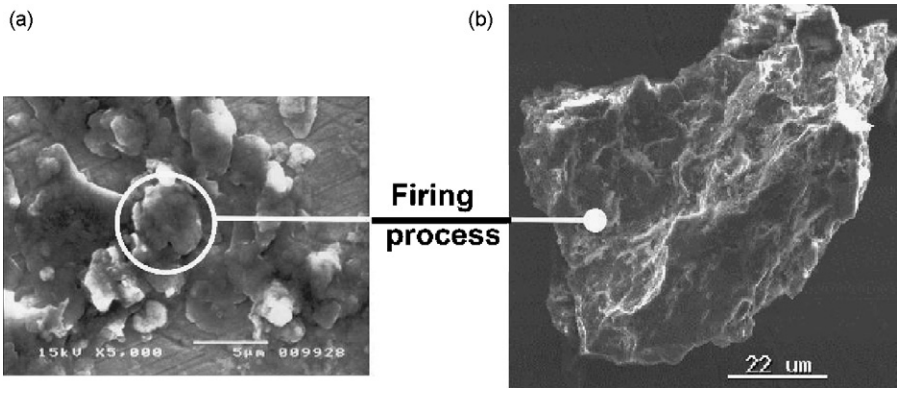

Fig. 11. SEM micrographs of (a) clay B and (b) a region of a fired brick sample.

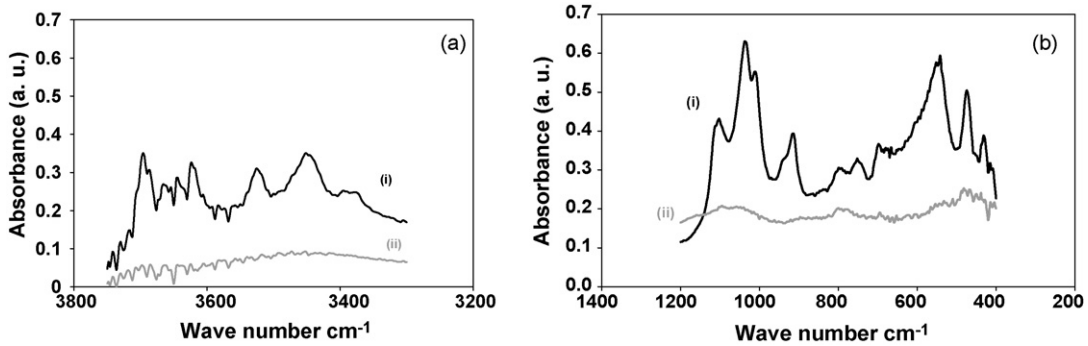

Fig. 12. (a and b) Details of the FTIR spectrum shown in Fig. 4. The plots show adsorbed water bands, structural water bands and groups containing either Al or Si of the adobe (i) and fired brick (ii) samples after leaching in water for 1 day.

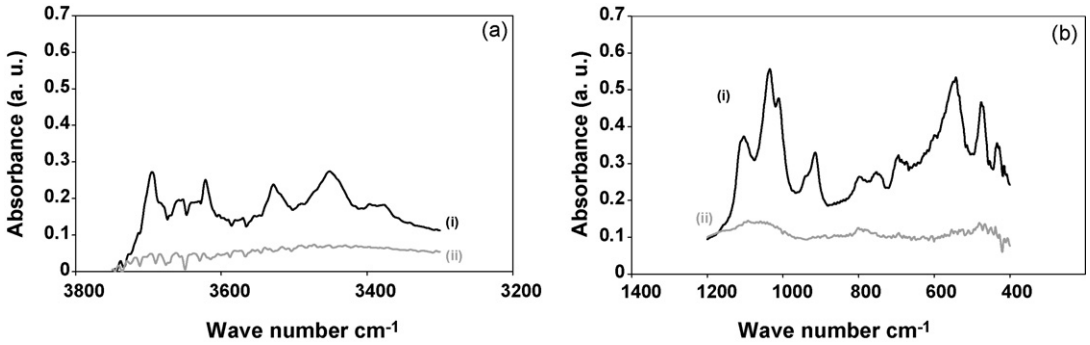

Fig. 13. (a and b) Details of the FTIR spectrum shown in Fig. 4. The plots show the adsorbed water bands, structural water bands groups containing either Al or Si of the adobe (i) and fired brick (ii) samples after leaching in Na-S solution for 1 day.

Table 2
Specific surface area (S_p), specific pore volume (V_p) and average pore diameter (D_p) for adobe upon leaching in water and $Na_2S_2O_5$ solution

	Adobe				
	Before leaching	1 day water	1 day Na–S solution	30 days water	30 days Na–S solution
S_p (m^2/g)	44	36	36	18	17
V_p (cm^3/g)	0.24	0.29	0.29	0.28	0.28
D_p (nm)	22	32	32	64	69

Table 3
Specific surface area (S_p), specific pore volume (V_p) and average pore diameter (D_p) for fired brick upon leaching in water and $Na_2S_2O_5$ solution

	Fired brick				
	Before leaching	1 day water	1 day Na–S solution	30 days water	30 days Na–S solution
S_p (m^2/g)	28	0.2	0.2	0.3	0.2
V_p (cm^3/g)	0.028	0.004	0.005	0.003	0.003
D_p (nm)	4	80	91	41	59

eliminated in the firing stage. In the region of the spectra between 3800 cm^{-1} and 3200 cm^{-1} (Figs. 12(a) and 13(a)) the absorption bands indicate the presence of free water. Again, these adsorption bands are more intense for the adobe sample (curve (i)).

Fig. 14 shows more pronounced water adsorption bands for the adobe sample after 30 days of exposure to water. This can be observed for instance for the Si–OH groups around 1200 cm^{-1}. This increase in the intensity of the water bands is also observed for the fired brick sample when submitted to the condition of 30 days immersion in water. Moreover, the fired brick sample after 30 days in Na–S solution (Fig. 15) shows significant reduction in the band intensities referred to the Si–O–Si (1034 cm^{-1}) and to the Si–OH bonds (1100 cm^{-1}).

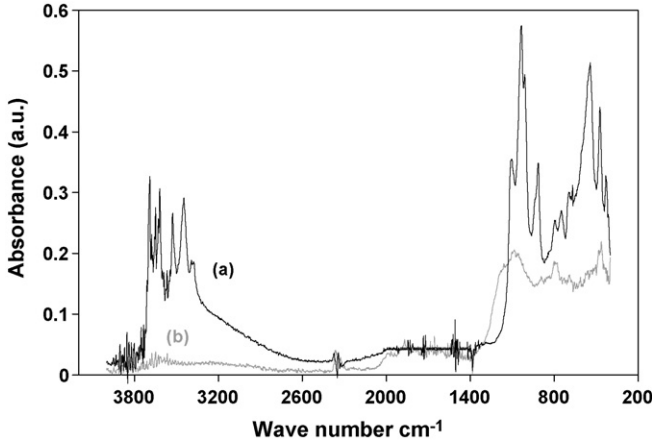

Fig. 14. FTIR spectra after leaching in water for 30 days for the adobe (a) and fired brick (b) samples.

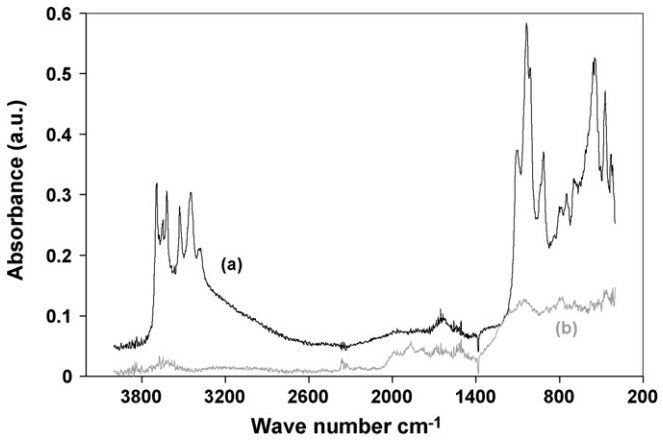

Fig. 15. FTIR spectra after leaching in Na–S solution for 30 days for the adobe (a) and fired brick (b) samples.

The smaller intensities of the water absorption bands for the fired brick sample in Figs. 14 and 15 suggest a more inert surface than that of adobe, which can be attributed to the different processing history of the samples. Adobe exhibits subtly different intensities between the bands referred to the Si–O–Si bonds (1079 cm^{-1}) and to the Al_2–OH bonds (914 cm^{-1}). This decrease in intensity is however more pronounced for the fired brick sample.

The results thus confirm that adobe and fired brick present different surface characteristics, with respect to both chemical nature and geometric parameters. The adobe surface shows poor durability to water, characterized by the presence of a large amount of OH groups and secondary bonding due to the absence of a firing stage. The fired brick is also a porous material and hydrophilic but the presence of primary bonds due to the firing stage results in lower porosity and less OH groups on its surface, thus exhibiting higher resistance to degradation in water.

4. Conclusions

The microstructure and degradation behaviour of two kinds of bricks, adobe and fired brick, and the clays that were used in their fabrication were evaluated. We observed that adobe is more susceptible to degradation by water-based solutions than fired brick. The high surface reactivity, associated with the large amount of OH groups, contributes to the degradation of both materials, but the weakening is more pronounced for the adobe sample, as shown by the results of leaching tests in water and in a $Na_2S_2O_5$ solution. The fired brick exhibited a significant increase in the average pore diameter after the first day of the leaching process, while its specific surface area decreased about three orders of magnitude. Its pore volume was also reduced and remained constant after 30 days of leaching for both leaching media tested. Future work should concentrate in investigating the mechanical properties of adobe in relation to fired brick, considering the lack of data in the literature, with the aim to assess the effect of degradation by water on adobe structural integrity.

Acknowledgments

The authors thank FAPEMIG and CNPq (Brazil) for the financial support.

References

[1] S. Somayaji, Civil Engineering Materials, Indian Institute of Technology/Prentice Hall, New Jersey, 1995.
[2] Construdobe, Sociedade de construção civil e ecológica. Algarve, Portugal, 2006. Website: www.construdobe.com.
[3] D.P. Bentz, D.A. Quenard, H.M. Kunzel, J. Baruchel, N.S. Martys, E.J. Garboczi, Microstructure and transport properties of porous building materials. II. Three-dimensional X-ray tomographic studies, Materials Structures 33 (2000) 147–153.
[4] M.A. Porta-gándara, E. Rubio, J.L. Fernández, Economic feasibility of passive ambient comfort in Baja California dwellings, Building and Environment 37 (2002) 993–1001.
[5] V. Médout-marère, H. Belarbi, P. Thomas, F. Morato, J.C. Giuntini, J.M. Douillard, Thermodynamic analysis of the immersion of a swelling clay, Journal of Colloid and Interface Science 202 (1998) 139–148.
[6] A.G. Kerali, Destructive Effects of Moisture on the Long-term Durability of Stabilized Soil Blocks, Development Technology Unit School of Engineering, University of Warwick, UK, 2000, p. 52.
[7] X. Xian-qing, F. Tong-xiang, S. Bing-he, Z. Di, T. Sakata, H. Mori, T. Okabe, Dry sliding friction and wear behavior of woodceramics/Al–Si composites, Materials Science and Engineering 342 (2003) 287–293.
[8] O. Altin, O.H. Ozbelge, T. Dogu, Effect of pH in an aqueous medium on the surface area, pore size distribution, density, and porosity of montmorillonite, Journal of Colloid and Interface Science 217 (1999) 19–27.
[9] E.L. Tavani, C. Volzone, Adsorption of sulphuric acid on smectite from acidic aqueous solutions, Cerâmica 45 (1999) 295.
[10] J. Van, T.K. Tokunaga, Partitioning of clay colloids at air–water interfaces, Journal of Colloid and Interface Science 247 (2002) 54–61.
[11] J. Baltrusaitis, C.R. Usher, V.H. Grassian, Journal of Physical Chemistry Chemical, Physics 9 (2007) 3011–3024.
[12] The Environmental Literacy Council, Washington, United States, 2007, Website: http://www.enviroliteracy.org/.
[13] S.N. Monteiro, C.M.F. Vieira, E.A. Carvalho, Matéria 10 (4) (2005) 537–542.
[14] W.L. Vasconcelos, Description of permeability in porous ceramics, Cerâmica 43 (1997) 120–123.
[15] R.S. Juang, S.H. Lin, K.H. Tsao, Mechanism of sorption of phenols from aqueous solutions onto surfactant-modified montmorillonite, Journal of Colloid and Interface Science 254 (2002) 234–241.
[16] A.J. Calabria, W.L. Vasconcelos, Structural evaluation of an adobe from Minas Gerais, in: Proceedings ICAM, ed. Applied Mineralogy: Developments in Science and Technology, vol. 1, Águas de Lindoia, Brazil, (2004), pp. 225–228.
[17] A.J. Calabria, W.L. Vasconcelos, Structure of an adobe from Tiradentes, Minas Gerais, in: Proceedings of the 48 Congresso Brasileiro de Cerâmica, Curitiba, (2004), pp. 5–59.
[18] A.R.R. Corrêa, V.H. Teixeira, S.P. Lopes, M.S. Oliveira, Ciência e Agrotecnologia 30 (3) (2006) 503–515.
[19] Website: http://www.greenhomebuilding.com/QandA/adobeQandA.htm#structural (accessed on 2/12/2007).
[20] C. Richard, S. Charles, A. Neville, in: Proceedings of the 6th International Conference on the Conservation of Earthen Architecture, Adobe 90preprints, Las Cruces, NM, USA, October 14–19, 1990.